



# FLUID INFLOW AND HEAT TRANSFER ENHANCEMENT: AN EXPERIMENTAL ANALYSIS OF NANOFLUIDS IN MINCHANNEL

Ameer Abed Jaddoa\*, Karema Assi Hamad, Arshad Abdul Jaleil Hameed

*Electromechanical Engineering Department, University of Technology, Baghdad, Iraq,00964*

## ABSTRACT

In the Heat Transfer process, many innovations were introduced aiming to obtain the most optimum behavior of the cooling process using nanofluids as coolant liquids. These nanofluids have gained much attention in cooling systems due to their special rheological and thermal performance. In this work, an experimental evaluation is conducted for nanofluids  $Al_2O_3$ ,  $SiO_2$ ,  $CuO$ ,  $ZnO$ , and  $TiO_2$  nanoparticles applied to a mini-channel. The nanofluid particles were entirely spread out in purified water (size of 15 nm) before being passed to the heat sink through a confined inflow channel. The obtained results showed that the achieved improvement rates are 25%, 20%, 15%, 10% and 5% by using 1-vol% nanoparticles in the distilled water. Also,  $Al_2O_3$  nanoparticles provided an outstanding performance compared to the other types. The reason is imputed to the fact that such an  $Al_2O_3$  has a thermal conductivity greater than the other nanofluids. Besides, the measured pressure of all nanofluid material types declined comparable to the pure water. Additionally, for  $Al_2O_3$ ,  $SiO_2$ ,  $CuO$ ,  $ZnO$ , and  $TiO_2$ , the recorded pressure was further dropped by 4%, 5%, 6%, 7% and 8%, respectively. The additional reduction in pressure was due to an increase in the density of nanofluids. The hypotheses of the conventional heat transfer process do not support the behavior achieved by the small number of nanoparticles of current work. Such a new behavior could be attributed to the generation of stochastic movements of both nanoparticles and micro heat carriers in the pure liquid (water), and it is in charge of enhancing thereof. Finally, despite the complexity of the suggested design, it can be added to existing methods in the literature.

**Keywords:** *Heat transfer enhancement, Pressure drop, Nanofluids, minichannel.*

## 1. INTRODUCTION

Some amount of electric power delivered to the electronic components is converted to thermal energy in their structure. Such thermal power needs to be effectively eliminated by proper cooling approaches. In another word, the remaining power in the elements has a negative impact on the component's efficient performance and therefore leads to damage thereof due to the high temperature. The accelerating evolution of technology resulted in the minimization of the entire electronic circuit size considerably. Since the heat increases per unit area, this, in turn, leads to inadequate available cooling methods. Generally, scientific researchers intend to increase the surface area of cooling fins made of different materials such as aluminium, and copper, exposed to air aiming to increase the cooling efficiency (Rahouadja, et al., 2019).

It is generally known that air and water are the components used in cooling processes. In this context, water is superior to air in terms of thermal conductivity capability, (about 25 times greater than the air), in which the thermal dissipation tends to be much quicker than that in air. Accordingly, this makes the processor to operate at significantly higher rates. According to the above-mentioned, scientific researchers have initiated their research to produce new liquids with high-cooling efficiency, (Kafel, et al., 2021), (Kaprawi et al., 2021), (Yun, et al., (2022) and (Zainab, et al., 2022)). Mixing the high conductivity material with the base fluid. In this context, several finned radiators of various designs and sizes were introduced in the literature. The objective here is to provide the highest quality cooling and effective operation. Furthermore, one of the produced materials is PHSS, which materials have high surface area/volume ratios and are under research production. On the other hand, regarding electronic systems, a plethora of research

in the literature, notably current works developing the liquids for working in such devices. An empirical study performed by (Pourfarzad, et al., 2018), analyzed the heat transfer and pressure reduction in a small-radiator sink fabricated from a porous material. In this work, alumina-water nanofluids with volumetric concentrations of 0.1%, 0.3%, and 0.5% were used. Also, the thermal sinks were fabricated from copper material that has two various pore concentrations of 15 PPI and 30 PPI and was mounted in the channel.

The results showed that an enhancement could be achieved by about 22%, and 26.4%, for 15 PPI and 30 PPI densities, respectively. In previous studies (Pourfarzad, et al., 2018), (Bayomy, et al., 2016), and Bayomy et al., 2017), the researchers introduced empirical works besides numerical analyses and sought to get an insight into the performance of using metal-foam heat-sink coolers for electronic cooling circuits. According to the procedures, for cooling the Intel core i7 processor, water was used with metal foam and then compared the performance was with the case of using a metal-foam heat-sink and nanofluids. Furthermore, the effect of channels number was also lighted in this study besides the number of aluminium fins. Concerning the obtained results, it was revealed that, in the first scenario, an enhancement could be achieved of 20% in heat transfer compared to the cleared channels.

Moreover, an improvement was obtained in the average Nusselt number by about 37% and 28%, respectively, upon Reynolds numerals, 601.3 and 210, using 0.2%  $Al_2O_3$  nanofluids compared to purified water. As far as the various channel numbers are concerned, in comparison, the recorded Nusselt numbers for four aluminium fins were higher than the three and five fins. The author in (Bayomy et al., 2020), adopted  $SiO_2/H_2O$  as nanofluids over the Reynolds number range of 4–22 based on various fluid densities of 0.2%, 0.5%, and 1%. The goal was to

\* Corresponding Author Email: [Ameer.A.Jaddoa@uotechnology.edu.iq](mailto:Ameer.A.Jaddoa@uotechnology.edu.iq)

analyze the cooling efficiency through the heat transfer performance inside the poly di-methyl siloxane mini-channels. The outcomes showed that the more reduction in the Reynolds number, the more the nanofluids are efficient in heat transfer.

In another study, based on two various morphologies and nanofluids  $\text{SiO}_2/\text{H}_2\text{O}$  and  $\text{ZnO}/\text{H}_2\text{O}$ , a bit of improvement in the Nusselt number was acquired, relative to the base fluid (Bayomy et al., 2017). While the research in Anoop (2012) introduced an empirical demonstration of a microchannel thermo-radiator utilizing distilled water besides nanofluids material such as  $\text{Al}_2\text{O}_3\text{-H}_2\text{O}$  and  $\text{CuO-H}_2\text{O}$ . Also, through tiny channels, the nanofluids were mixed with a volume fraction ranging from 0.1-0.5-vol% as coolant-fluid, of a heat sink. The results showed that 31% and 29% improvements were accomplished in terms of heat transfer factor utilizing  $\text{Al}_2\text{O}_3\text{-water}$  and  $\text{CuO/water}$  nanofluids, respectively, compared to the distilled water. Finally, a reduction in the sink base temperature of 3 °C was reported as a comparison between these two scenarios. In adopted  $\text{TiO}_2$  as the nanofluid for the cooling process and investigated the hydrodynamic features besides the heat transfer experimentally. The three-channel configuration was in a wavy shape. The density of nanometer-sized particles was 0.006, 0.008, 0.01, and 0.012-vol%. Upon comparing the results with distilled water in heating environments with power values of 25 W, 35 W, and 45 W, the results demonstrated that the performance of nanometer-sized particles was superior the pure water in terms of heat transfer. Moreover, the more the heating energy, the more the degradation in nanometer-sized particle characteristics.

Concerning the base heat degree, it was noted that the lowest recorded wall base temperature and highest improvement of 0.012% nanometer-sized particle concentration were 33.85 °C and 40.57%, respectively. These recorded values were based on a wavelength of 5 millimetres and amplitude of 0.5 millimetres related to a Reynolds value of 894 at a heating power of 25 W. The inflow rate and pressure reduction can be The inflow rate and pressure reduction can be inferred by pumping power which is related to the heat sink with the lowest wavelength. Additionally, it was found that the channel's wavelength variation has a dominant impact on the heat transfer feature of the heat sink concerning the dimensions of the microchannel (Ferrouillat et al., 2013) .

In the literature on  $\text{Al}_2\text{O}_3$  and  $\text{CuO-water}$  nanofluids, for electronic cooling, the authors in (Raisoni et al. 2015), investigated the heat performance of various inflow shapes using a microchannel heat sink. The range of the highest and lowest values of the Nusselt number was 4.49%–12.5% specified for  $\text{Al}_2\text{O}_3\text{-water}$  nanofluids while it was ranging between 5.77% and 16.01% for  $\text{CuO-water}$  nanofluids, with 0.1% vol for both types. Experimentally, the results were validated and evaluated with the results that already existed analytically and numerically in the literature. In a prior study (Muhammad et al., 2019), the author reported that the highest PF factor obtained with a Reynolds value of 1900 was 2.6 throughout the experiment. Furthermore, these values were achieved with wavy microchannels. Additionally, the result revealed that there is an opposite relationship between Nusselt quantity and pressure besides the increase in proportional waviness in the laminar and transitional inflow system. Such a study was carried out based on a microchannel heat sink utilizing nanometer-sized particles and purified water.

A systematic literature review was conducted of studies in (Nada et al., 2022) , (Dominic et al., 2015) and (Sultan et al., 2021). Experimentally and based on various criteria, for instance, particle density and their sizes, mix-fluid heat degree, and Brownian movement, the influence of nanoparticle fluids on heat conductivity were examined. In reviewing the literature (Sultan et al., 2021) data were found on the association between various volume fractions of  $\text{Al}_2\text{O}_3$  nanoparticles. The recorded Nusselt and Reynolds numbers were 9.5% and 132, respectively, for nanoparticles fluid concentration of 0.04%. Noted that the number 9.5% indicates the percentage of increase relative to the deionized purified water. In comparison, it was discovered that the

percentage enhancement was 5.8% for nanoparticle fluid  $\text{Al}_2\text{O}_3$  work with a 10-nm channel diameter and volume fraction of 0.04 superior to the deionized purified water. This in turn led to a reduction in thermal resistance by 2.9%. In (Sultan et al., 2021) , recalling the (Mingzheng et al., 2022) , the more concentration of nanoparticles, the more efficient output energy, the more reduction in thermal resistance and logarithmic average heat degree difference in heat sinks. In this context, compared to purified water, a 28.7% improvement in the Nusselt value was measured at the heat temperature of 33.86C with 0.01 vol.% of nanoparticle fluid concentration.

The research (Muhammad et al. 2022) showed a comparison between the two scenarios, distilled water against nanoparticles fluid. The work stated that irrespective of the microchannel shapes, the recorded thermal resistance was reduced with an increase in the average Nusselt number. This enhancement is attributed to the  $\text{CuO}$  nanoparticle fluid. Alternatively, such a study was further extended for  $\text{CuO-water}$  and  $\text{Al}_2\text{O}_3\text{-water}$  nanofluids. The performance of  $\text{CuO}$  was superior to the  $\text{Al}_2\text{O}_3$ . In this regard, the work in (Yusuf et al. 2022) reported that there is a variation in the minimum entropy production rate level relative to the nanoparticle size in nanofluids. Moreover, in another study (Sameh et al., 2022) ,the heat sink with the mini fin method provided a worse performance compared to the modified hexagonal fin microchannel heat sink despite the lower heat transfer zone. In a previous study (Nadaab et al. 2022) , the authors investigated the effect of an axial electric field on inflow acceleration. In this context, the outcomes showed that fluid velocity declined because of applying the transverse magnetic field. Furthermore, in the presence of both fields the transverse and axial, the transverse field has a positive impact on the fluid velocity, in other words, the speed rose up to a specific level and then declined. While in another study, the more increased the Nusselt value and the more the heat transfer mechanism becomes dominant, the more probability of convection occurring. As the authors anticipated, the nanoparticle fluid type  $\gamma\text{-Al}_2\text{O}_3/\text{water}$  has a lower impact than  $\text{MWCNT-Fe}_3\text{O}_4/\text{Water}$  (Hybrid Abdelkadir 2018).

It was noted that the maximum and minimum bound to represent the Highest average of heat transfer and the most useful case of heat degree uniformity, respectively (Khwaja et al., 2018) .Compared between microchannel and micro gap, for the same interior factors, it was revealed that the heat transfer was more consistent in the microchannel than in the gap. Additionally, to attain an inflow uniform distribution of nanofluids, the pressure must be constant and equilibrium at both the interiors of the channels and gaps (Farhad et al., 2020).

The available hypotheses about the heat transfer process in nanoparticle fluids indicate inadequate information regarding the characteristics since this is a new type of nanofluid. As a consequence, it is important to implement a significant range of precise and dedicated empirical for all available nanoparticle fluids and their circumstances to establish a bank of data to be used for analytical investigations. From another perspective, much-drawn attention has been paid recently to the cooling of energy harvesting techniques, for instance, the generator operates based on a solid-state device, and benefits from the available enhancement approaches. As explained aforementioned above, one cooling method needs the support of the scientific community with a database of the cooling TEGs utilizing nanoparticle fluids.

Thus, the current paper provides a conceptual theoretical framework for developing heat transfer operations by adopting two passive approaches, minichannels and nanofluids. In this vein, an empirical investigation is conducted on the study and analyzes the impact of various nanoparticle fluids  $\text{Al}_2\text{O}_3$ ,  $\text{SiO}_2$ ,  $\text{CuO}$ ,  $\text{ZnO}$ , and  $\text{TiO}_2$  on transfer of heat using a tiny exchanger of heat . The size of nanoparticles used was 15nm which have been scattered in the purified water pursuing to prepare suspension a stable with a fraction of volume 1%. Finally, comprehensive comparisons were made in terms of heat transfer and pressure between the two scenarios.

## 2. EXPERIMENTAL SETUP

This part is devoted to illustrating the empirical procedures of examining heat transfer by convection of the nanoparticle fluid inflow besides the apparatuses utilizing the tiny channel as present in Figure 1 and 2. Using copper 360 alloys, the tiny channels were fabricated to the heat sink. The dimensions of such a model are 34 millimetres times 33 millimetres and 5 millimetres in thickness. Figure 2 exhibits the prototype of the model. This figure illustrates the components which can be indicated by consistent arrays of 8 fins and 9 rectangular cross-section microchannels designed with 0.5 millimetres hydraulic diameter. The experimental system under investigation comprise a cylinder filled with 99.7% of pure nanofluids. The heated ammonia gas (orange) used for the refrigerant regime is compressed by the compressor.

For the cooling process, a number of coils were utilized to cool the ammonia gas, which condensed indicated in figure 1b by dark blue to be converted to liquid form at high pressure. Such high-pressure gas flows through a tiny hole of the expansion valve while the pressure at the other side of the hole is low to enable the compressor to discharge gas out of this region. This, in turn, leads to the ammonia gas being at high heat degrees, which are passed to an expansive room to become gaseous at a low temperature of  $-27^{\circ}\text{F}$ . Such a heating/cooling process is repeated several times over the operational work time. Additionally, in a cooling system, the coolant unit is deemed significant besides the type of cooling gas used. In this regard, the criteria for adopting a gas include flexibility of temperature control of gas (up/down), environment-friendly, low density, and considering the gas workability at high temperatures besides its cost.

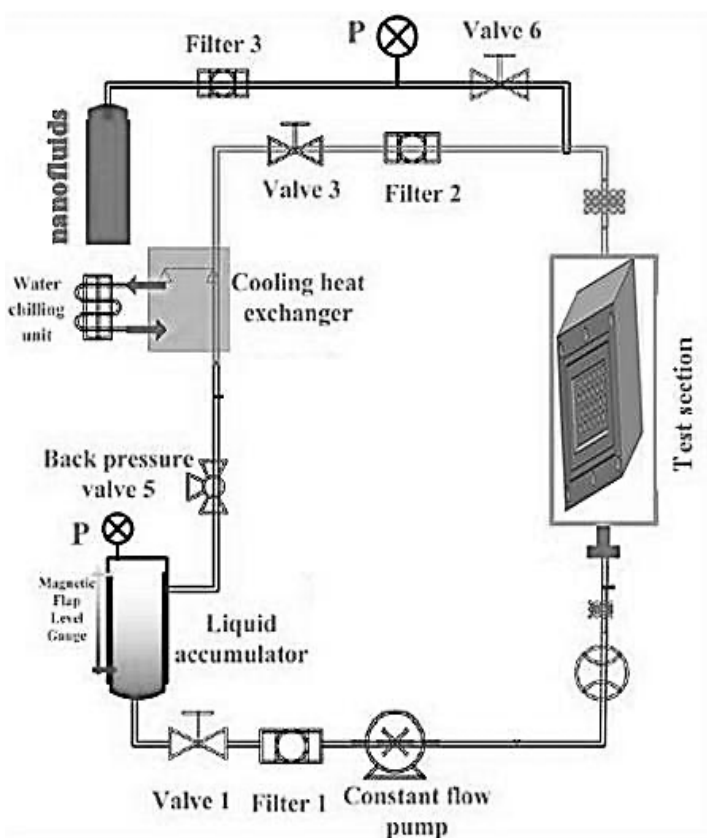


**Fig. 1** Experimental setup of (schematically)

It is worth mentioning that such a coolant has the advantage of having less impact on the regime in terms of its ability to electrical insulation, resistance to erosion, and work with a chemically inert gas. To control the flow rate on the two sides, it was adopted a classic needle

valve has the feature of the ability to operate at high pressure. Generally speaking, such a valve can operate with a pressure greater than 200 bar with a temperature range of  $-10$ – $200^{\circ}\text{C}$ , and lower than  $31/2$  of the whole open. Noted that all components were fabricated from stainless steel to the name but a few handles, springs, and mounting screws. Several versatile device (thermal and pressure) sensors were employed as independent measurement devices with the ability to measure the entire volume through a built-in totalizer measurement. Additionally, the differential pressure type 5210–7 was utilized to measure the differential mass flow at any line point, and it works within a range of  $0$ – $30$  L/min with 2% precision. Furthermore, the precise volume can be measured using the totalizer relying on the trigger pressure and temperature. Along with the above instruments, another apparatus was also mounted called a data recorder embedded within the model, pretending to record the information, preserve and display it on a certain meter device. At the end of the whole carbon dioxide system experimental test, different information was recorded and preserved simultaneously, such as the flow of nanofluids, gas volume and pressure.

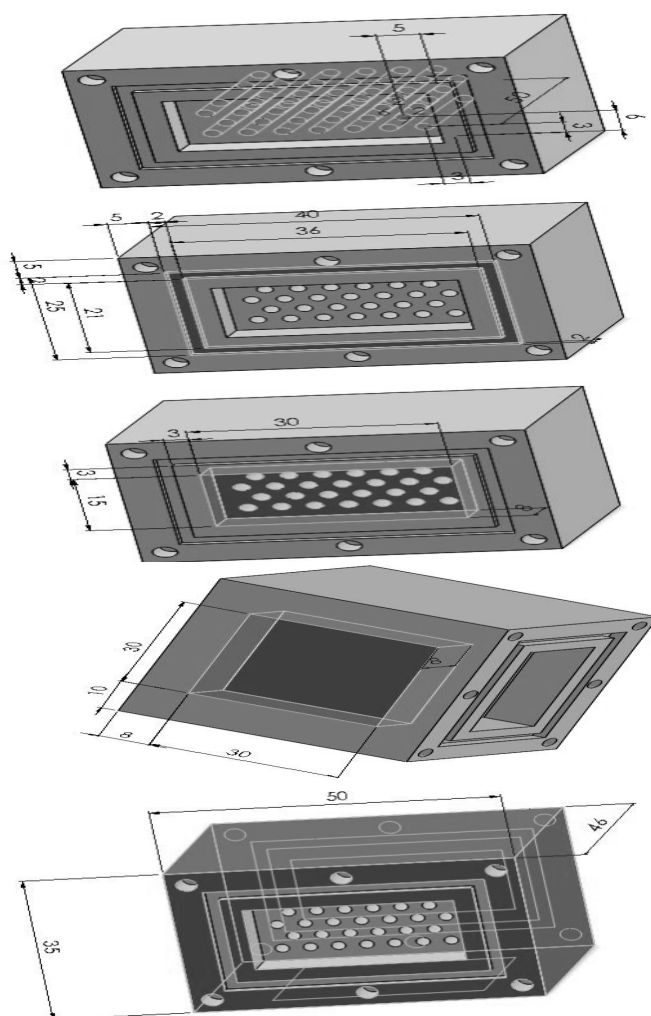


**Fig. 2** Experimental setup (test section)

The colour and touchable screen of the system has the ability to show and conserve four readings, simultaneously. The FLO-Sight program was set up to drive the gas inflow meter, which was interfaced with a computer which was used to set the system data besides the data exposing. Additionally, an analogy linear temperature sensor type Lm35 was employed with a scale measurement of 10 mv reads 1 degree Celsius.

In the current work, 2 degree Celsius was proportionate to Arduino's voltage till the maximum value was reached. It is worth noting that the Arduino Uno microcontroller employed for the temperature control process operates with a voltage range of 0–5, proportional to the heat fluctuation and it can memorize reading data from 0–1023 as a 10-bit. The type k sensor is commonly used in many applications was adopted for readings ranging from -200 to 1350 °C or -330 to 2460 °F.

The k-type thermocouple meter is a linear sensitive device made for chrome–alum with 41  $\mu\text{V}/^\circ\text{C}$ . This type of meter is composed of two semiconductors interfaced by wire. The operation idea of such a device relies on the thermoelectric impact, which is proportional to the voltage and heat degree measured. Regular thermocouples are broadly utilized as heat-degree measurement meters. Moreover, since this type of thermocouple is manufactured from nickel, it is suitable for temperature measurements. At 185 degrees (Curie point), a deflection emerges in the output.

The outer body is made of carbon steel. The purpose is for the filtration process of nanoparticle fluids and it is designed to operate up to 100 bar. Given that the material optimum of Nichrome is composed of Chromium 20 % and Nickel 80 %, this qualified it to work at high heat degrees, and this in turn prevents the possibility of damage of wires besides the prevention of breaking cases. Also, it characterizes as an anti-oxidant material along with it has the prohibition of production layer of chromium oxide. Noted that the Nichrome heating segment can carry about 6.8 Amper and 1500 Watt with a length of 10 meters. In relation to AC transformer 520T-10 – 14 lbs with 10 A, the operating voltage is up to 130 output volute, 110 volts of input terminals, 10 amper output current, 3 pins with 3 sockets at the output. A friendly environment material such as Cellulose was employed for thermal isolation.

Its contents of recycled paper fibres are about 85% and the remainder comprises retardants of fire such as ammonium sulphate or boric acid. The combustion products are lower due to it has no oxygen because of their compressed material, that is to say, such materials are more likely to be applied in fire-fighting. Due to the electrical conductivity ability, ductile and malleable, the pure copper of 99.5% and 29 atomic number has been used to fabricate the parts of the test rig.

### 3. APPARATUSES AND EXTRACTED DATA

The empirical model was equipped with different measurement apparatuses to record and memorize the heat degree, pressure, inflow velocity, and interior electric temperature. Table 1 shows the values of such parameters. The experimental components were adopted so as to reduce the uncertainty of measured variables such as heat flux, tiny channel wall heat degree, mass fluid heat degree, and heat transfer factor in the transducer section. The entire statistical analysis of the test scenario data is shown in Table 2. Under these conditions, the temperature values must be adopted in one decimal figure. This is because of the dubiety of single-decimal place thermocouples. For more convenience, many important recorded values were adopted to describe such calculations.

### 4. NANOFLUID PRODUCTION

The nanoparticle fluids  $\text{Al}_2\text{O}_3$ ,  $\text{SiO}_2$ ,  $\text{CuO}$ ,  $\text{ZnO}$ , and  $\text{TiO}_2$  all mixed with water, were organised based on two procedures. First, for about fifteen hours and at 200 kHz, using distilled water, the nanoparticles were dispersed in an ultrasonic bath (AC220V UK) before being mounted appropriately as shown in Figure 3. In the test containers, the mixtures were stored for several days as shown in Figure 4.

**Table 1** The apparatuses utilized in the empirical test with their uncertainty measurements calculations

Instrument	Location	Model and Serial	Uncertainty	Span
Press.Trans.	Pump Outlet	PX-309-3KGI 071814DO42	$\pm 0.25\%$ FS	0 to 3000 PSI
Press.Trans.	Test Section Inlet	MMA2.5KV10 P4COT3A5E43 2727	$\pm 0.20\%$ FS	0 to 2500 PSI
Thermocouple	Test Section Flux Meter	KMQSS-02U-6	$\pm 1.1^\circ\text{C}$ OR $\pm 0.4\%$	-200 to 1250 $^\circ\text{C}$
Thermocouple	Test Section Inlet/Outlet	TMQSS-062U-6	$\pm 0.5^\circ\text{C}$ OR $\pm 0.4\%$	-250 to 350 $^\circ\text{C}$
Mass Flow Meter	Supercritical Fluid Loop	TCM-0325-FK-SGSS-CADS1305525	$\pm 0.1\%$ Rdng	0 to 325 kg hr-1
Wattage Meter	Test Section Flux Meter	GW5-103E16060602	$\pm 0.2\%$ Rdng	0 to 100 W

**Table 2** Statistical analysis of measured variables for scenario P = 8, G = 50  $\text{kg m}^{-2} \text{s}^{-1}$ , q = 50  $\text{W cm}^{-2}$ ,  $T_{in} = 60^\circ\text{C}$

Variable	$X_m$	n	T	$T_{Cl,v}$	p
$m'$ ( $\text{kg s}^{-1}$ )	1.436 $\times 10^{-3}$	1400	2.972 $\times 10^{-4}$	1.785	$\pm 1.121 \times 10^{-5}$
$P_{in}$ (MPa)	7.5	1400	53.50	1.785	$\pm 1.31$
$T_{in}$ ( $^\circ\text{C}$ )	48.6	1400	0.31	1.785	$\pm 0.01$
$T_{ex}$ ( $^\circ\text{C}$ )	75.0	1400	0.07	1.785	$\pm 0.02$
$T_1$ ( $^\circ\text{C}$ )	240.5	1400	0.60	1.785	$\pm 0.01$
$T_2$ ( $^\circ\text{C}$ )	351.9	1400	0.34	1.785	$\pm 0.02$
$T_3$ ( $^\circ\text{C}$ )	212.2	1400	0.61	1.785	$\pm 0.03$
$T_4$ ( $^\circ\text{C}$ )	352.8	1400	0.45	1.785	$\pm 0.04$
$T_5$ ( $^\circ\text{C}$ )	259.8	1400	0.28	1.785	$\pm 0.01$
$T_6$ ( $^\circ\text{C}$ )	368.0	1400	0.93	1.785	$\pm 0.02$
Wattage (W)	94.179	1400	0.55	1.785	$\pm 0.01$

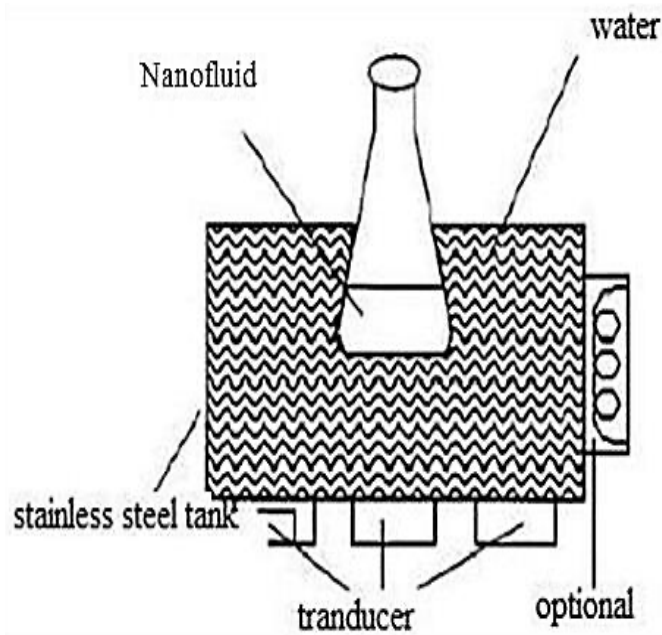


**Fig. 3** ultrasonic bath (AC220V UK)

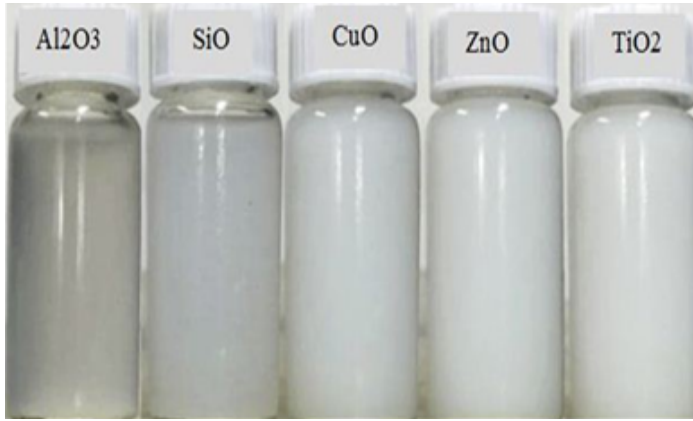


**Fig. 4** The as-prepared nanofluids

Table 3 illustrate the thermo-physical characteristics of purified water besides the nanoparticle fluids types.

**Table 3** The properties of nanoparticles and distilled water

Properties	Al <sub>2</sub> O <sub>3</sub>	SiO <sub>2</sub>	CuO	ZnO	TiO <sub>2</sub>	Distilled water
$\mu$ (kg/ms)	-	-	-	-	-	10 <sup>-3</sup>
$\rho$ (kg/m <sup>3</sup> )	3600	2560	6500	5800	4250	996.5
$k$ (W/mK)	36	1.5	18	9.6	8.95	0.613
$C_p$ (J/kg K)	765	730	540	735	686	4181

In what follows are the mathematical expressions of nanofluids, such as the specific heat capacity and viscosity utilizing the two-phase mixture expressions .

Density of nanofluids :

$$\rho_{nano} = \varphi \times \rho_p + (1 - \varphi)\rho_b \quad (1)$$

where the fraction of volume  $\varphi$  nano-particles in a fluid of base is presented as:

$$\varphi = V_p \times V_b^{-1} \quad (2)$$

The density, volume fraction, and specific heat capacity of the base liquid are the main factors that affect the specific heat capacity of nanofluids. As shown below.

$$C_{p\ nano} = [C_{p\ b} \times (1 - \varphi)\rho_b + (\varphi \times \rho_p \times C_{p\ p})] \times \rho_p^{-1} \quad (3)$$

The useful density of nanofluids with a nanoparticle is given as:

$$\mu_{nano} = \mu_b \times [1 - 18.6 \times (\frac{d_p}{d_b})^{-0.9} \times \varphi^{-1.25}]^{-1} \quad (4)$$

where  $d_{pis}$  molecules of the diameter in the base fluid and is computed as:

$$d_b = [(3 \times M) \times (\pi \times N \times \rho_b)^{-1}]^{0.356} \quad (5)$$

where N is the number of Avogadro, M is the weight of molecular of the fluid base.

The conductivity of thermal nanofluids is calculated by:

$$k_{nano} = (k_b k_p + (n k_b - k_b) - (\varphi n k_b k_p - \varphi k_b k_p) \times (k_b k_p + n k_b k_p - k_b) + (\varphi k_b - \varphi k_p)^{-1} \quad (6)$$

where n is the factor of shape is calculated by:

$$n = 6 \varepsilon^{-1} \quad (7)$$

And  $\varepsilon$  is attributed to the sphericity of the particles. For spherical-shaped nanoparticles,  $n = 2$ . The calculated properties of the thermal nanofluids are shown in Table 4:

**Table 4** The calculated properties of nanofluids

Properties	Al <sub>2</sub> O <sub>3</sub> -water	SiO <sub>2</sub> -water	CuO-water	ZnO-water	TiO <sub>2</sub> -water
$\mu$ (kg/ms)	0.001245	0.003482	0.004111	0.4324	0.0011342
$\rho$ (kg/m <sup>3</sup> )	1150.36	1200.56	1189.76	1099.42	1080.76
$k$ (W/mK)	0.856	0.8789	0.7922	0.7442	0.732
$C_p$ (J/kg K)	4316.23	4311.67	4289.22	4250.83	4212.23

The heat of absorbed by the fluid is calculated as:

$$Q = m c_p T_{out} - m c_p T_{in} \quad (8)$$

The temperatures of the fluid mean ( $T_m$ ) is the properties physical of thermo used for computing the of the coolants:

$$T_m = 1/2(T_{in} + T_{out}) \quad (9)$$

The provided heat by AC power supply is calculated as:

$$Q = V \times I \quad (10)$$

where V is voltage and I is electric current.

Heat transfer coefficient of convection is calculated as:

$$Q = \Delta T_{con.} \times h \times A_{con.} \quad (11)$$

where  $A_{con.}$  is the heat transfer of convection area and  $\Delta T_{con.}$  (con.) is the temperature difference between the fluid  $T_{fluid}$  and wall  $T_{wall}$  temperature which is calculated as:

$$\Delta T_{con.} = T_{wall} - T_{fluid} \quad (12)$$

Reynolds number is calculated by :

$$Re = D_H \times u_m \times \rho \times \mu^{-1} \quad (13)$$

where  $u_m$  is the velocity mean of the fluid through micro-channels and  $D_H$  is the diameter of hydraulic.

The number of Nusselt is a significant parameter of dimensionless in transfer of the heat subjects that is defined by :

$$Nu = D_H \times h \times k_{nano}^{-1} \quad (14)$$

Thermal resistant consists of three parts: conduction, convection, and capacity resistant that are defined as following

$$R_{total} = [(H \times k^{-1} \times A^{-1})_{conduction}] + [(T_w - T_m) \times Q^{-1}] - (H \times k^{-1} \times A^{-1})_{convection}] + [(T_m - T_{in}) \times Q^{-1}]_{capacity} \quad (15)$$

where H is the thickness of heat sink, A is transfer of the heat area and Q is heat power.

Total thermal resistance can be calculated as:

$$R_{total} = (T_{wall} - T_{inlet}) \times Q^{-1} \quad (16)$$

## 5. RESULTS AND DISCUSSION

In this section, the outcomes of the convection heat transfer process are exhibited using purified water mixed with Al<sub>2</sub>O<sub>3</sub>, SiO<sub>2</sub>, CuO, ZnO, and TiO<sub>2</sub> nanofluids through tiny channels. In this regard, a comparison was



conducted based on experimental and theoretical based equations of coolant for six various Re numbers and a fraction of the volume 1%. In the heat transfer functioning, the underside of the heat sink was supplied with a constant power of 50 W. For six different Reynolds numbers, the measured wall temperature of various working fluids such as purified water,  $Al_2O_3$ ,  $SiO_2$ , CuO, ZnO, and  $TiO_2$ -water, is illustrated in Figure 5.

The experimental findings indicated that the wall heat degree dropped because of mixing nanofluids with base fluid. Furthermore, the more increasing the Reynolds number increases, the more decline the wall temperature; Wherein such behaviour was recorded for all types of liquids. Besides, at the Reynolds number =3000, employing nanofluid type  $Al_2O_3$ - water, a decline in the wall temperature of about 18.93% was monitored.

Due to decreasing in the thermal boundary layer thickness which has an opposite relationship with the Reynolds number, leads to an increase in the efficiency of absorption from the heated wall. The measured declining heat degrees using  $SiO_2$ , CuO, ZnO, and  $TiO_2$  nanofluids were 12.53, 11.44, 10.86 and 10.12, respectively, at identical Reynolds numbers in comparison to water. A decrease in the thermal boundary layer thickness, which has an opposite relationship with the Reynolds number, leads to an increase in the efficiency of absorption from the heated wall.

The measured declining heat degrees using  $SiO_2$ , CuO, ZnO, and  $TiO_2$  nanofluids were 12.53, 11.44, 10.86, and 10.12, respectively, at identical Reynolds numbers compared to water. Moreover, it can be demonstrated that the  $Al_2O_3$  nanofluids have greater heat transfer efficiency, heat absorptivity notably thermal conductivity than  $SiO_2$ , CuO, ZnO, and  $TiO_2$  due to the heat transfer rate of alumina, as shown in Figure 6. The tiny channel heat sinks thermal resistance deems as a significant factor since it indicates thermal performance. Thus, the lower the thermal resistance, the higher the cooling performance of the heat sink. Figure 7 illustrates the thermal resistance of nanofluids. it can be seen that the more increase in Reynolds number, the more the thermal resistance decreases for all coolants.

Additionally, in comparison, distilled water exhibits a higher thermal resistance than nanofluids, this, in turn, implies the advantage of nanofluids over purified water. As appears in Figure 7, for instance, the reduction percentages of thermal resistance are 8.52%,6.34,5.67, 4.32, and 3.32 for  $Al_2O_3$ ,  $SiO_2$ , CuO, ZnO, and  $TiO_2$  nanofluids, respectively, recorded at Reynolds number=3000.

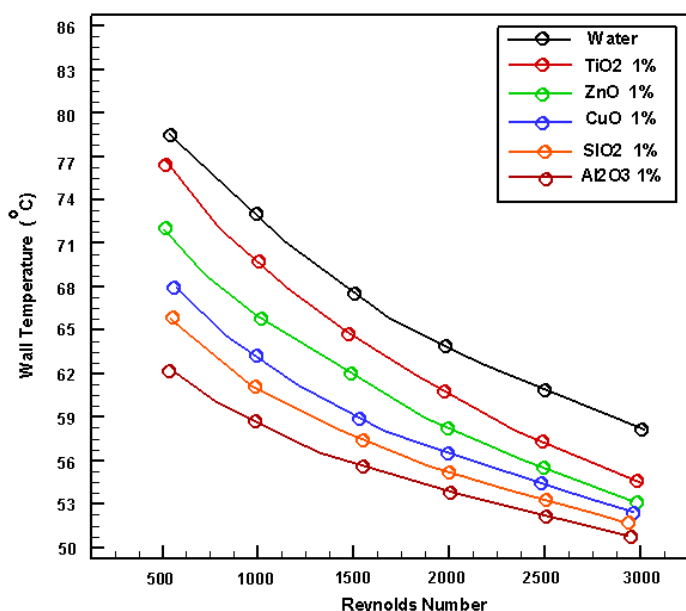


**Fig. 5** Comparison of nanofluids and distilled water, plotted as wall temperature and Reynolds number

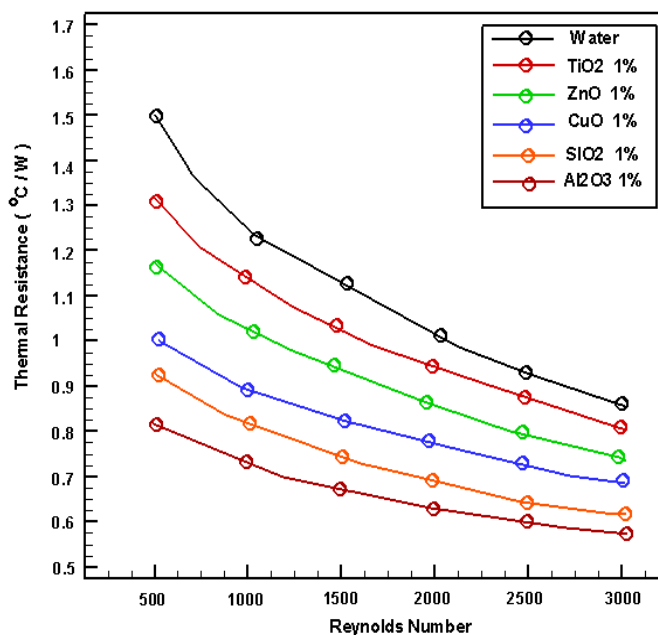


**Fig. 6** Thermal resistance comparison between distilled water and nanofluids

As previously stated, distilled water has the lowest heat transfer factor than nanofluids. Figure 8 presents the percentage improvement of the thermal performance. For example, 25%,20%,15%,10% and 5%, for  $Al_2O_3$ ,  $SiO_2$ , CuO, ZnO, and  $TiO_2$ , nanofluids. Given that the Nu number indicates the transfer of heat rate concerning the surface in dimensionless form, it can be said that the higher the Nusselt number values, the higher the heat transfer for pure water and nanofluids, as shown in Figure 9. Furthermore, the greater the Reynolds number, the greater the Nusselt number. In other words, adopted nanofluids could increase heat transfer rates. Additionally, Nusselt number values of  $Al_2O_3$  nanofluids are greater than those of other working fluids. This is attributed to the properties of  $Al_2O_3$  in terms of thermal characteristics, which increase the Nu number. Besides, the pressure deems as a significant indication concerning the fluid flow and heat transfer. Such a factor signifies sufficient pumping power to move the coolant fluid inside the microchannels. Thus, based on different Reynolds numbers values applied to all working fluids, Figure 10 presents the declined pressure values. The outcomes revealed that, the more increasing Reynolds value, the more reduction in pressure drop for distilled water and both nanofluids. Besides, the pressure deems as a significant indication concerning the fluid flow and heat transfer. Such a factor signifies sufficient pumping power to move the coolant fluid inside the microchannels. Thus, based on different Reynolds number values applied to all working fluids, figure 7 presents the declined pressure values.

The outcomes revealed that, the more increasing Reynolds value, the more reduction in pressure drop of distilled water and both nanofluids. In this vein, the negative remarked indication is the pressure drop in nanofluids and this is a negative case characteristic of nanoparticles fluids. The reason for such behaviour can be attributed to incremented in nanofluids density compared to the purified water. It can be seen that the percentages of pressure reductions were 2.95,2.83,2.63,2.31, and 2.22% for  $Al_2O_3$ ,  $SiO_2$ , CuO, ZnO, and  $TiO_2$  nanofluids, respectively, at the Reynolds number of 3000, with distilled water. For more convincing, the results were compared with the results in the literature as in (1-18), at the Nusselt number for pure water. Taking into consideration various concentrations, nanoparticle fluids, the size of the microchannel, power, and Reynolds value.

In this context, the Nusselt value for a rectangular microchannel in which the walls were heated all over around was achieved. It was noted

that a comparable argument between both the current work results and the results in the literature. as illustrated in Figure 10.

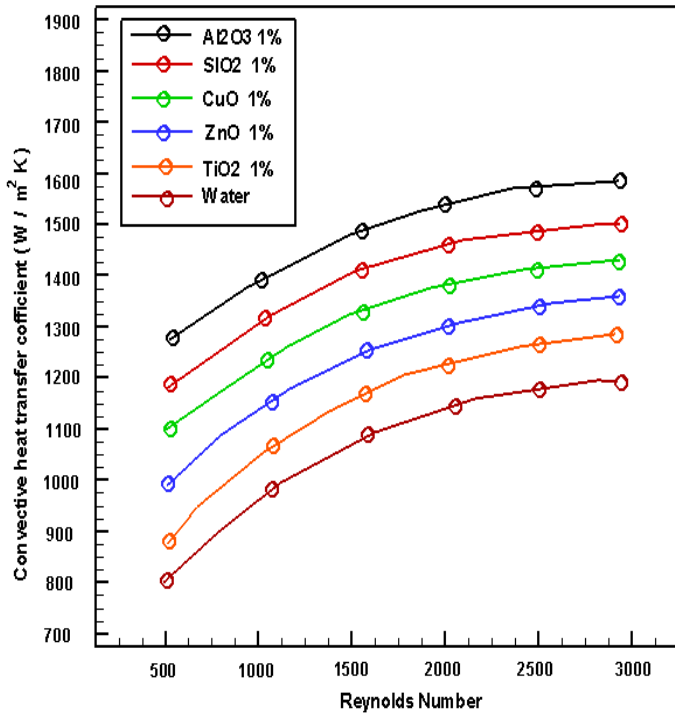


Fig. 7 Heat transfer coefficient of the convective comparison between nanofluids and water.

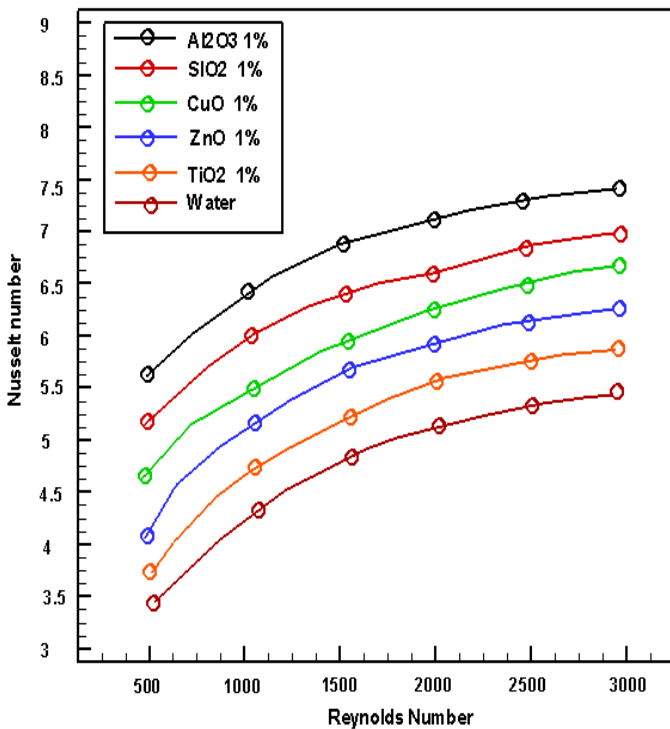


Fig. 8 Nu number comparison between distilled water and based-water nanofluids .

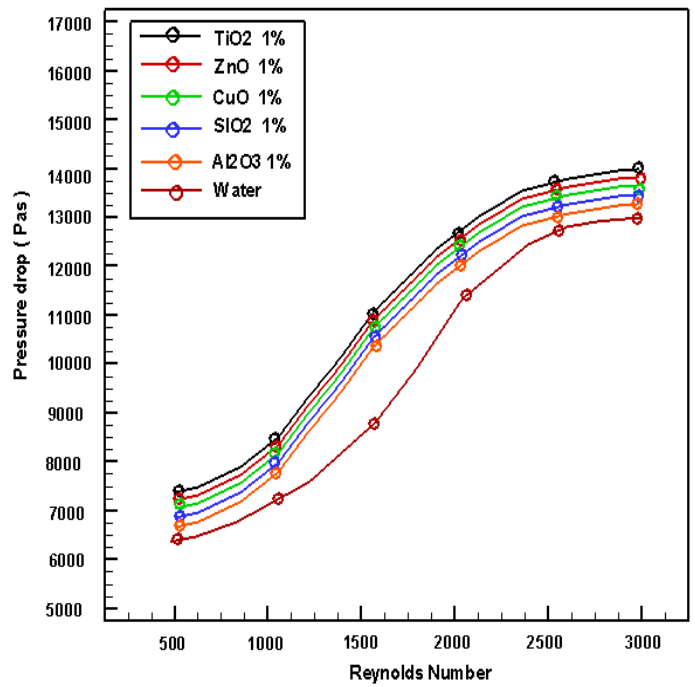


Fig. 9 Pressure drop comparison between nanofluids and distilled water

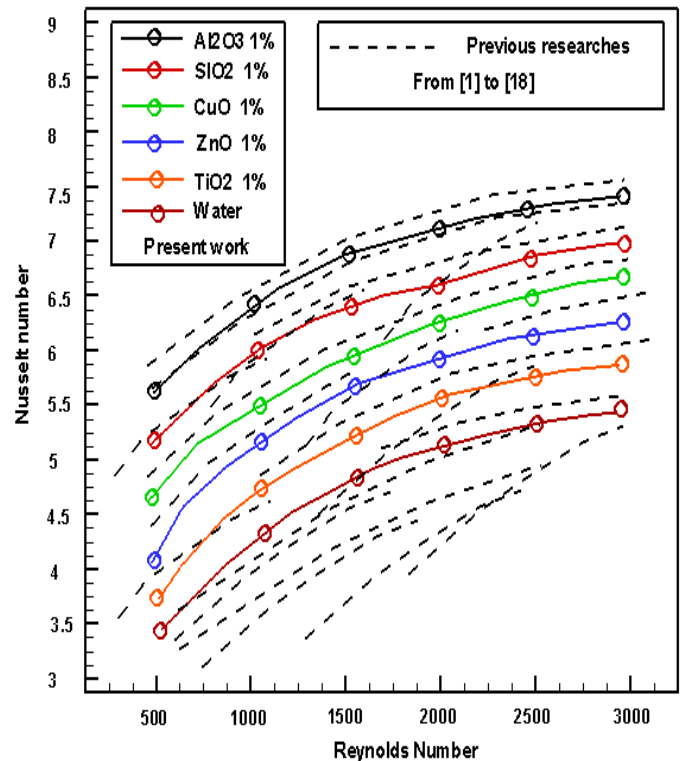


Fig. 10 Comparisons between present work and previous researches

## 6. CONCLUSIONS

The present study was designed to investigate heat transfer and pressure drop behaviours for different scenarios in terms of pure water, Al<sub>2</sub>O<sub>3</sub>, SiO<sub>2</sub>, CuO, ZnO, and TiO<sub>2</sub> experimentally, and by employing a copper-

made microchannel heat sink. A 50 W heat flux power was adopted on the downside of the heat sink.

A fractional of nanofluids of 1% was used as an ultrasonic bath. The results revealed that in terms of thermal performance, Al<sub>2</sub>O<sub>3</sub> nanofluids outperform the other kinds and pure water by a percentage of 25%. Also, with Al<sub>2</sub>O<sub>3</sub>, the minimal recorded wall temperature was 50 at Reynolds number=2800.

Additionally, heat transfer is improved by 20%,15%,10% and 5% in the case of using SiO<sub>2</sub>, CuO, ZnO, and TiO<sub>2</sub> nanofluids compared to base water. The use of nanoparticle fluids leads to reduce thermal resistance and pressure, wherein the main negative feature was regarding the pressure. Finally, the recorded percentages of reduction of pressure were 2.95, 2.83, 2.63, 2.31, and 2.22, respectively, compared to the purified water.

## ACKNOWLEDGEMENTS

This research was supported by the University of Technology- Iraq

## NOMENCLATURE

A	convection heat transfer area (m <sup>2</sup> )
D	Diameter (m)
d	Diameter of molecules
G	Mass Heat flux (m <sup>-2</sup> s <sup>-1</sup> )
M	Weight of molecular
N	Number of Avogadro
n	Factor of shape
Q	Convection heat transfer (W)
q	Heat flux (W cm <sup>-2</sup> )
R	Resistance of Thermal (°C W <sup>-1</sup> )
T	Temperature (°C)
V	Voltage (V)
I	Current (A)
μ	Viscosity (kg/ms)
ρ	Density (kg/m <sup>3</sup> )
k	Thermal conductivity (W/mK)
C <sub>p</sub>	Specific heat transfer (J/kg K)
φ	volume fraction
ε	Sphericity of particles
ΔT	difference of Temperature (°C)
ΔP	difference of Pressure (bar)
Re	Reynolds number
Nu	Nusselt number
m'	Flow rate of Mass (kg s <sup>-1</sup> )

Subscript	
in	inlet
nano	nanofluids
p	Particle
b	Base fluid
m	mean
out	outlet
con	convection
w	wall
f	fluid
H	hydraulic

## REFERENCES

Anoop K., Sadr R., Yu J., KanS. g, Jeon S. and Banerjee D.,2012," Experimental study of forced convective heat transfer of nanofluids in a microchannel", *Int. Commun. Heat Mass Transfer* 39 , 1325–1330. . <https://doi.org/10.1016/j.icheatmasstransfer.2012.07.023>

Bayomy A.M.; Saghir Z.; Yousefi,T. Electronic Cooling Using Water Flow in Aluminum Metal Foam Heat Sink2016," Experimental and

Numerical Approach",*Int. J. Therm. Sci.*, 109, 182–200. <https://doi.org/10.1016/j.ijthermalsci.2016.06.007>

Bayomy A.M.; Saghir, Z.,2017," Experimental Study of Using -Al<sub>2</sub>O<sub>3</sub>- Water Nanofluid Flow Through Aluminum Foam Heat Sink" Comparison with Numerical Approach",*Int. J. Heat Mass Transf.* 107, 181–203. [10.1016/j.ijheatmasstransfer.2016.11.037](https://doi.org/10.1016/j.ijheatmasstransfer.2016.11.037)

Bayomy A.M.; Saghir, Z.,2020," Thermal Performance of Finned Aluminum Heat Sink Filled with ERG Aluminum Foam: Experimental and Numerical Approach" *Int. J. Energy Res*, 44, 4411–4425. <https://doi.org/10.1002/er.5217>

Bayomy A.M. and Saghir, Z. ,2017, "Experimental and Numerical Study of the Heat Transfer Characteristics of Aluminium Metal Foam (with/without channels) Subjected to Steady Water Flow",*Pertanika J. Sci.Tech.*,25,221246.<https://www.researchgate.net/publication/313391187>

Belhadj A., Rachid S., and Bouchenafa R., 2018, "Numerical investigation of forced convection of nanofluid in microchannels heat sinks", *Journal of Thermal Engineering*, 5(4), 2263-2273. <https://jten.yildiz.edu.tr/storage/upload/pdfs/1636700346-en.pdf>

Dominic A., Sarangan J., Sivan S., and Devahdhanush V. S. ,2015, "An Experimental Investigation of Wavy and Straight Minichannel Heat Sinks Using Water and Nanofluids", *Journal of Thermal Science and Engineering Applications*7(3), 31-44. <https://doi.org/10.1115/1.4030104>

Ferrouillat S., Bontemps A., . Poncet O, O., and Soriano J.-A. Gruss,2013," Influence of nanoparticle shape factor on convective heat transfer and energetic performance of water-based SiO<sub>2</sub> and ZnO nanofluids", *Appl. Therm. Eng.*, 51 , 839–851. [10.1016/j.applthermaleng.2012.10.020](https://doi.org/10.1016/j.applthermaleng.2012.10.020)

Ghobena Z. K., and Hussein A. K., 2022," natural convection in a partially heated parallelogrammatical cavity with v-shaped baffle and filled with various nanofluids", *Frontiers in Heat and Mass Transfer*, 18(6),1-9. <https://dx.doi.org/10.5098/hmt.18.6>

Ghadiri P.E., Behrangzade K. and Ashjaee M., 2018," Experimental Investigation of Heat Transfer and Pressure Drop of Alumina–Water Nano-Fluid in a Porous Miniature Heat Sink. Exp.", *Heat Transfer*,31, 495–512. [DOI: 10.36884/jafm.11.SI.29413](https://doi.org/10.36884/jafm.11.SI.29413)

Hao Y., Lv S. and Wu S.,2022, "experimental research on the heat transfer characteristics of nanofluids in crude oil heatin furnaces", *Frontiers in Heat and Mass Transfer*, 18(3),1-11. <https://dx.doi.org/10.5098/hmt.18.3>

Jianqiang M. Y. , Jin D. ,W. Lei Chenb , Sabev P., V. and Jiří Jaromír Kleměšc,2022," Investigation on thermal performance of nanofluids in a microchannel with fan-shaped cavities and oval pin fins", *Energy* , 260, 125000. <https://doi.org/10.1016/j.energy.2022.125000>

Nada S.A., El-Zoheiry R.M. Elsharnoby M. and Osman O. S. ,2022," Enhancing the thermal performance of different flow configuration minichannel heat sink using Al<sub>2</sub>O<sub>3</sub> and CuO-water nanofluids for electronic cooling: An experimental assessment", *International Journal of Thermal Sciences* , 181, 38-50. . [DOI: 10.1016/j.ijthermalsci.2022.107767](https://doi.org/10.1016/j.ijthermalsci.2022.107767)

Moghanlou F. S., Noorzadeh S., Ataei M., Vajdi M., As M. S., and Esmaeilzadeh E.,2020, "Experimental investigation of heat transfer and pressure drop in a minichannel heat sink using Al<sub>2</sub>O<sub>3</sub> and TiO<sub>2</sub>- water nanofluids", *Journal of the Brazilian Society of Mechanical Sciences and Engineering* ,42(315) ,3-11. [DOI: 10.1038/s41598-022-13519-0](https://doi.org/10.1038/s41598-022-13519-0)

Mohammeda K. A., Saleemb A. M. and alabdeen Obaida Z. H.,2021," numerical investigation of nusselt number for nanofluids flow in an inclined cylinder", *Frontiers in Heat and Mass Transfer*, 16( 20),1-12. [DOI: 10.5098/hmt.16.20](https://doi.org/10.5098/hmt.16.20)



Raisoni G. H. and Shelke R., 2015, "experimental study on improvement of heat transfer of minichannel heat sink using nanofluids", *Physics Engineering*, 8 (12) , 1–16. <https://www.semanticscholar.org/author/G.-H.-Raisoni/52374342>

Sameh A., Nadaab R.M. , El-Zoheirya , M. Elsharnoby and O.S.Osmana 2022, "Enhancing the thermal performance of different flow configuration minichannel heat sink using Al<sub>2</sub>O<sub>3</sub> and CuO-water nanofluids for electronic cooling: An experimental assessment", *International Journal of Thermal Sciences*, 181, 107767, <https://doi.org/10.1016/j.ijthermalsci.2022.107767>

Sajid M. U. , Ali H. and Sufyan H. A. ,2019," Experimental investigation of TiO<sub>2</sub>–water nanofluid flow and heat transfer inside wavy minichannel heat sinks", *Journal of Thermal Analysis and Calorimetry*,137(5),20-35  
<https://link.springer.com/article/10.1007/s10973-019-08043-9>

Sahim K., . Puspitasari D and Nukman,2021," experimental study of convective heat transfer of alumina oxide nanofluids in triangle channel with uniform heat flux", *Frontiers in Heat and Mass Transfer*, 16(22),1-9. DOI: 10.5098/hmt.16.22

Sajid M. U., Ali H. M. and Bicer Y.,2022," Exergetic performance assessment of magnesium oxide–water nanofluid in corrugated

minichannel heat sinks: An experimental study", *Energy research*,46(8), <https://doi.org/10.1002/er.6024>

Sultan K. F., Jabal M. H. and Ameer Abed Jaddoa, 2021," Energetic and Exergetic Assessment of Spiral Heat Exchanger Using Mineral and Oxide Mineral Oil Nanofluid", *International Journal of Heat and Technology*, 39(2), 531-540. <https://doi.org/10.18280/ijht.390223>

Sultan K. F., Anead H. S. and Ameer Abed Jaddoa,2021," Energetic and Exergetic Assessment of the Cooling Efficiency of Automobile Radiator Using Mono and Hybrid Nanofluids", *International Journal of Heat and Technology*, 39(4), 1321-1327. . <https://doi.org/10.18280/ijht.390431>

Sultan K. F., Jabal M. H. and Ameer Abed Jaddoa,2021," Performance Assessment of the Heat Exchanger with and without a Coating of Hybrid Nanoparticles the User Cooling System in Solar Heating Systems", *International Journal of Heat and Technology*, 39(5), 1460-1468. <https://doi.org/10.18280/ijht.390507>

Zarita R. and Hachemi M., 2019," numerical investigation and analysis of heat transfer enhancement in a microchannel using nanofluids by the lattice boltzmann method" *Frontiers in Heat and Mass Transfer*, 12( 5 ),1-8. <https://dx.doi.org/10.5098/hmt.12.5>